A Lateral Regulator Diode with Field Plates for Light-Emitting-Diode Lighting *

Yi-Tao He(何逸涛)**, Ming Qiao(乔明)**, Lu Li(李路), Gang Dai(代刚), Bo Zhang(张波), Zhao-Ji Li(李肇基)

State Key Laboratory of Electronic Thin Films and Integrated Devices, University of Electronic Science and Technology of China, Chengdu 610054

(Received 29 March 2016)

A lateral current regulator diode (CRD) with field plates is proposed and experimentally demonstrated. The proposed CRD is based on the junction field-effect transistor (JFET) structure. A cathode field plate is adopted to alleviate the channel-length modulation effect and to improve the saturated I–V characteristics. An anode field plate is induced to achieve a high breakdown voltage V_B of the CRD. The influence of the key device parameters on the I–V characteristics of the lateral CRD are discussed. Experimental results show that the proposed CRD presents good I–V characteristics with a high V_B about 180 V and a low knee voltage (V_k) below 3 V. Furthermore, the proposed CRD has a negative temperature coefficient. The well characteristic of the proposed CRD makes it a cost-effective solution for light-emitting-diode lighting.

PACS: 71.20.Mq, 73.61.Cw, 73.40.Qv, 72.20.Fr DOI: 10.1088/0256-307X/33/9/097101

In recent years, light emitting diodes (LEDs) have been widely used in automotive, industrial and lighting applications due to their advantages, such as high luminous efficacy, long lifetime, small size, and low power consumption.[1–3] Usually, conventional current regulators for driving LEDs are realized by integrated circuits, which are complex, expensive and noisy.[4,5] Recently,the current regulator diode (CRD) has been used as a simple and economical solution for driving LEDs, which is based on the junction field-effect transistor (JFET) structure. A lateral JFET structure has a simple manufacturing process while it takes up a large area since a long drift region and a long channel length are needed to withstand high applied voltage and to achieve saturated I–V characteristics. Although a vertical JFET structure may save area, it suffers from poor saturation characteristics due to the channel-length modulation effect.[6–10] We have reported a vertical CRD with trench cathode based on double epitaxial layers to improve the I–V characteristics.[11] However, it increases the difficulty of the manufacturing process and somehow reduces the consistency of the device performance.

In this Letter, a lateral CRD with field plates is proposed and demonstrated. A cathode field plate is adopted to alleviate the channel-length modulation effect. An anode field plate is induced to achieve a high breakdown voltage (V_B) without increasing the drift length. The influence of the key device parameters on I–V characteristics are discussed. Experiments show that the proposed lateral CRD presents good I–V characteristics with a wide regulating range and is successfully applied to LED lighting.

Figure 1(a) shows schematically the cross-sectional view of the proposed lateral CRD. The n^+ source and p^+ gate of the JFET structure are shortened to form the cathode of the CRD. A cathode field plate is adopted, which forms the JFEF region 2 between the cathode field plate and P-sub. Moreover, an anode field plate is induced to achieve a high V_B without increasing the drift length. Here, L_1 and L_2 are the lengths of the cathode and anode field plate, respectively, L_d is the length of the n-drift region, and L_{ch} and W_{ch} represent the channel length and width, respectively. With the increase of the anode voltage (V_A), electrons flow from the cathode to the anode through the n-well and the anode current (I_A) increases. When the channel pinches off, I_A becomes saturated. Since the depleted region beneath the cathode field plate will expand with the increase of V_A, the resistance of JFET region 2 is increased, which shields the influence of V_A on the channel region (i.e., JFET region 1). Therefore, the channel-length modulation effect is alleviated. Figure 1(b) shows the schematic I–V characteristics of the proposed lateral CRD, which can realize a regulating current (I_S) in a wide voltage range. Here V_k represents the knee voltage, which is the anode voltage when $I_A = 0.8I_S$. In applications, the CRD is in series with LEDs and two or more CRDs can be in parallel for higher current ability as shown in Fig. 1(c).

In this study, the device structures were obtained from TSUPREM4 and then imported into MEDICI for device simulation.[12,13] Here, L_d has slight effect on the current capability and is fixed as 18 μm to ensure V_B of the CRD. Figure 2(a) shows the simulated I–V characteristics of CRD with different L_1. The value of V_B of CRD will decrease slightly with the increase of L_1. However, the I–V characteristic is more saturated. Without the cathode field plate (i.e.,

*Supported by the National Natural Science Foundation of China under Grant No 61376080.
**Corresponding author. Email: yitaohe@126.com; qiaoming@uestc.edu.cn
© 2016 Chinese Physical Society and IOP Publishing Ltd

$L_1 = 0\,\mu m$), the CRD suffers poor and unsaturated I–V characteristics due to the channel-length modulation effect. Figures 2(b) and 2(c) show the flowlines and depletion edges of the CRD without cathode field plate and with $L_1 = 9\,\mu m$. The current path in the JFET region 2 becomes narrower by adopting cathode field plate, which increases the resistance and shields the influence of V_A on the channel region. Therefore, channel-length modulation effect is alleviated and the I–V characteristic is improved. When $L_1 = 7\,\mu m$, the proposed CRD can achieve not only saturated I–V characteristics but also a high V_B of 207 V.

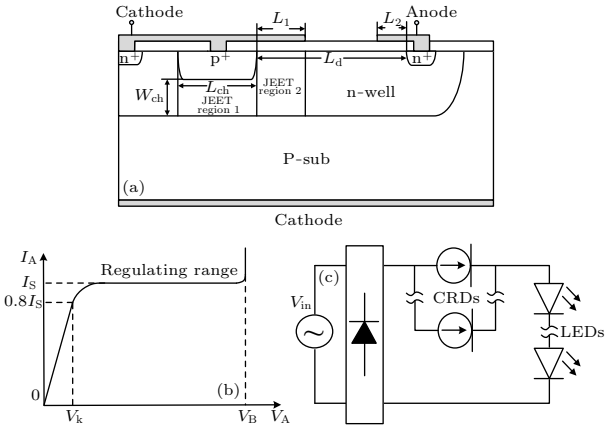

Fig. 1. (a) Schematic cross-sectional view of the proposed lateral CRD. (b) Schematic I–V characteristics of the CRD. (c) The typical application circuit of the CRD for LED lighting.

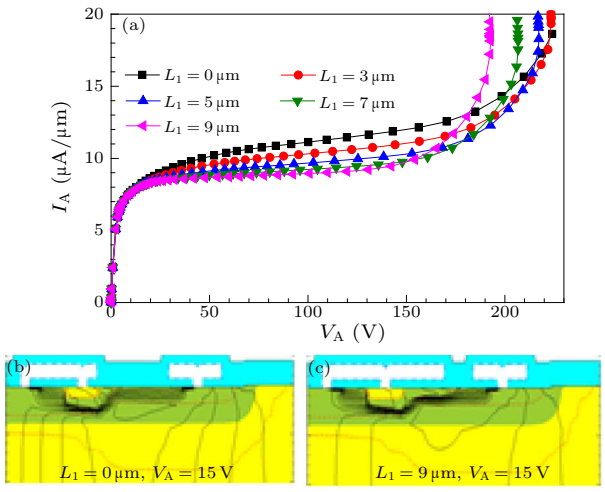

Fig. 2. (a) Simulated I–V characteristics of the CRD with different L_1. The flowlines and depletion edges of the CRD (b) without cathode field plate and (c) with $L_1 = 9\,\mu m$.

Figures 3(a) and 3(b) show the simulated I–V characteristics of the CRD with different L_2 and L_{ch}, respectively. Without the anode field plate (i.e., $L_2 = 0\,\mu m$), V_B is only 172 V. By adopting anode field plate, V_B can greatly increase to about 217 V when $L_2 = 3\,\mu m$ and 5 μm. Moreover, the anode field plate does not affect the current characteristics of the device. Figure 3(b) shows that as L_{ch} increases from 4 μm to 10 μm, I_A decreases greatly, which also makes V_B slightly increase. Furthermore, at longer L_{ch}, the CRD can achieve more saturated I–V characteristics due to the fact that the channel-length modulation effect is alleviated at longer L_{ch}.

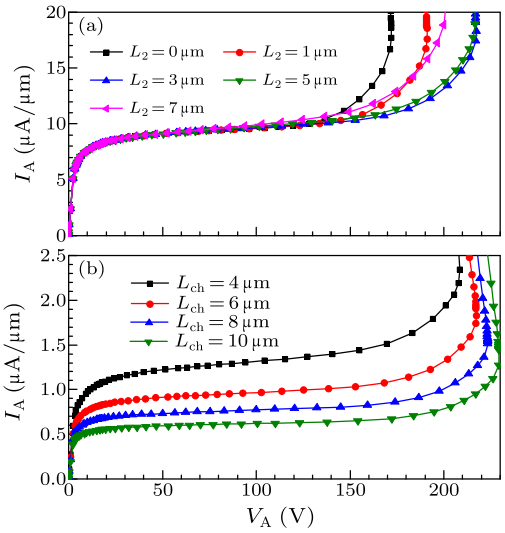

Fig. 3. Simulated I–V characteristics of the CRD with different (a) L_2 and (b) L_{ch}.

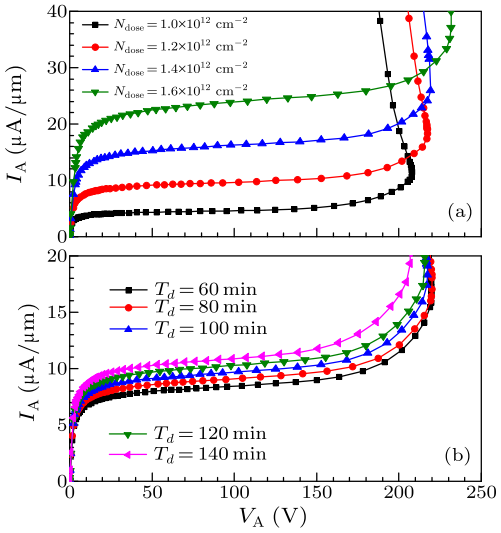

Fig. 4. Simulated I–V characteristics of the CRD with different (a) N_{dose} and (b) T_d.

The forming of the n-well is determined by an implanted impurity dose (N_{dose}) and the main thermal diffusion time T_d, and can greatly affect the performance of the CRD due to the fact that it affects the width and the doping concentration of the channel. Figures 4(a) and 4(b) show the simulated I–V characteristics of the CRD with different N_{dose} and T_d, respectively. As N_{dose} increases from $1 \times 10^{12}\,cm^{-2}$ to $1.6 \times 10^{12}\,cm^{-2}$, V_B increases from 208 V to 232 V. At the same time, I_A increases greatly more than 5 times due to the fact that the doping concentration

in the channel increases. Figure 4(b) shows that with increasing the thermal diffusion time from 60 min to 140 min, I_A increases and V_B decreases slightly from 220 V to 207 V.

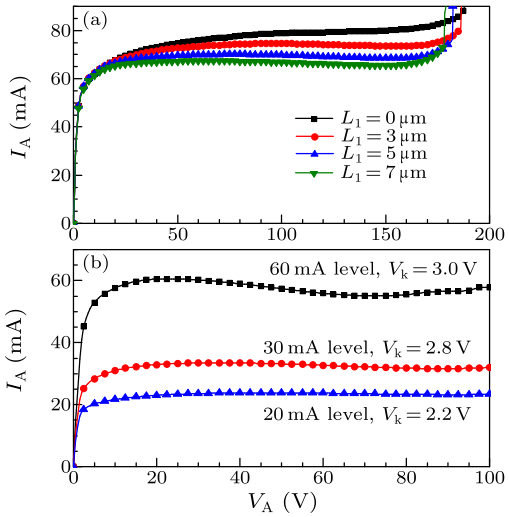

Fig. 5. (a) Experimental I–V characteristics of the CRD with different L_1. (b) Experimental I–V characteristics of the packaged CRDs with different current levels (20 mA, 30 mA and 60 mA).

Based on the above discussion, $L_1 = 7\,\mu m$, $L_2 = 3\,\mu m$, $L_{ch} = 6\,\mu m$, $N_{dose} = 1.2 \times 10^{12}\,cm^{-2}$ and $L_d = 18\,\mu m$ are chosen in the experiment. The junction depth of p+ and n-well are designed as about 0.5 µm and 3.5 µm, respectively. Figure 5(a) shows the experimental I–V characteristics of the proposed CRD with different L_1. By adopting the cathode field plate, the channel-length modulation effect is alleviated and more saturated I–V characteristic can be achieved. The CRD shows a wide stable regulating current and a V_B about 180 V when $L_1 = 7\,\mu m$, which makes it have good ability of voltage surge suppression. To satisfy various current level LED application, the CRD with different regulation current levels are designed by changing the thermal diffusion time of n-well. Figure 5(b) shows the experimental I–V characteristics of the packaged CRDs with different current levels, in which I_S is defined as the current at $V_A = 15$ V. With the increase of I_S, V_k increases correspondingly. Here V_k of the proposed CRD with 30 mA level is only about 2.8 V and the dynamic resistance is as high as 6 kΩ.

Figure 6(a) shows the measured regulating current degradation with time of the packaged CRD. The regulating currents will tend to saturation after 60 s. The current degradation is larger at higher current level CRD. The 30-mA-level CRD shows only 7.7% degradation. Figure 6(b) shows the experimental I–V characteristics of the packaged 30-mA-level CRD under different environment temperatures. The CRD has a negative temperature coefficient since the carrier mobility will decrease with the increase of temperature. The negative temperature coefficient characteristic is helpful to protect LEDs from thermal runaway at high voltages and currents.

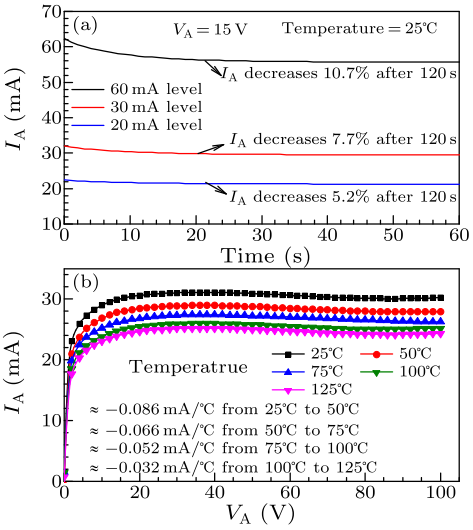

Fig. 6. (a) Current degradation with time. (b) Experimental I–V characteristics of the packaged 30-mA-level CRD under different environment temperatures.

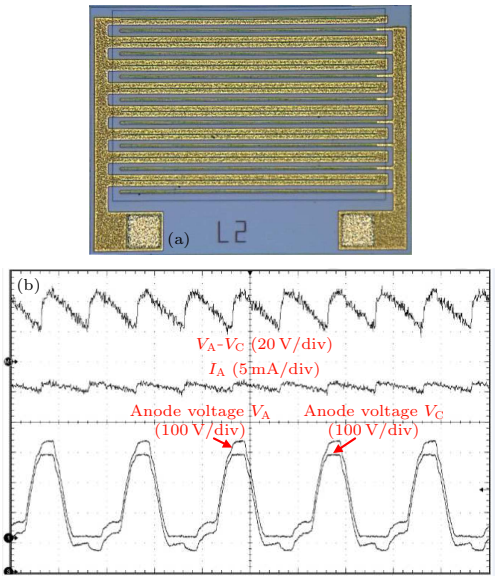

Fig. 7. (a) Micrograph of the proposed lateral CRD. (b) Measured waveforms of the 30-mA-level CRD in LED lighting application (220 V AC input, in series with 78 LEDs: 3.3 V, 30 mA).

Figure 7(a) shows the micrograph of the proposed CRD, which has a small active device size of $600 \times 850\,\mu m^2$. Figure 7(b) shows the measured waveforms of the 30-mA-level CRD in LED lighting applications. The CRD is in series with 78 LEDs (3.3 V, 30 mA). Under the 220 V ac input, the CRD is able to withstand a voltage range from 16 V to 50 V and the current fluctuation is only from 29.0 mA to 31.8 mA. Small size, wide regulating voltage range, high dy-

namic resistance and negative temperature coefficient make the proposed CRD a cost-effective solution for LED lighting.

In summary, a CRD with field plate technology is proposed and experimentally demonstrated. A cathode field plate is adopted to alleviate the channel-length modulation effect and to improve the saturated I–V characteristics. An anode field plate is induced to achieve a high $V_{\rm B}$ of CRD. The influence of the key device parameters on the I–V characteristics are discussed and optimized. CRDs of different regulation current levels with a $V_{\rm B}$ about 180 V, a $V_{\rm k}$ below 3 V and negative temperature coefficient are experimentally realized and are successfully applied to LED lighting.

References

[1] Loo K H, Lun W K, Tan S C, Lai Y M and Tse C K 2009 *IEEE Trans. Power Electron.* **24** 2967

[2] He S M, Luo X D, Zhang B, Fu L, Cheng L W and Wang J B 2012 *Chin. Phys. Lett.* **29** 127802

[3] Ma L, Shen G D, Liu J P, Gao Z Y, Xu C and Wang X 2014 *Chin. Phys.* B **23** 118507

[4] Loo K H, Lai Y M, Tan S C and Tse C K 2011 *IEEE Trans. Power Electron.* **26** 1943

[5] Kim J K, Lee J B and Moon G W 2014 *IEEE Trans. Ind. Electron.* **61** 4649

[6] Wong W W and Liou J J 1992 *IEEE Trans. Electron Devices* **39** 2576

[7] Chang J, Kapoor A K, Register L F and Banerjee S K 2010 *IEEE Trans. Electron Devices* **57** 1846

[8] Ozawa O 1980 *IEEE Trans. Electron Devices* **27** 2115

[9] Mihaila A, Udrea F, Rashid S J et al 2006 *IEEE Int. Symp. Power Semiconductor Devices ICs* (Naples, Italy, 4–8 June 2006) p 1

[10] Hao Y, Kuniss U, Kittler G et al 2013 *IEEE Int. Symp. Power Semiconductor Devices ICs* (Kanazawa, Japan, 26–30 May 2013) p 143

[11] He Y T, Qiao M, Dai G et al 2015 *IEEE Int. Symp. Power Semiconductor Devices ICs* (Hong Kong, 10–14 May 2015) p 157

[12] MEDICI Manuals, Synopsys Inc., Fremont 2004

[13] TSUPRE M-4 Manuals, Synopsys Inc., Fremont 2007